Coulomb Force Directed Single and Binary Assembly of Nanoparticles from Aqueous Dispersions by AFM Nanoxerography

Etienne Palleau,[†] Neralagatta M. Sangeetha,[†] Guillaume Viau,[†] Jean-Daniel Marty,[‡] and Laurence Ressier[†,*]

[†]Université de Toulouse, LPCNO, INSA-CNRS-UPS, 135 Avenue de Rangueil, 31077 Toulouse, France, and [‡]Université de Toulouse, IMRCP, UMR CNRS 5623, 118 Route de Narbonne, 31062 Toulouse, France

ABSTRACT We present a simple protocol to obtain versatile assemblies of nanoparticles from aqueous dispersions onto charge patterns written by atomic force microscopy, on a 100 nm thin film of polymethylmethacrylate spin-coated on silicon wafers. This protocol of nanoxerography uses a two-stage development involving incubation of the desired aqueous colloidal dispersion on charge patterns and subsequent immersion in an adequate water-soluble alcohol. The whole process takes only a few minutes. Numerical simulations of the evolution of the electric field generated by charge patterns in various solvents are done to resolve the mechanism by which nanoparticle assembly occurs. The generic nature of this protocol is demonstrated by constructing various assemblies of charged organic/inorganic/metallic (latex, silica, gold) nanoparticles of different sizes (3 to 100 nm) and surface functionalities from aqueous dispersions onto charge patterns of complex geometries. We also demonstrate that it is possible to construct a binary assembly of nanoparticles on a pattern made of positive and negative charges generated in a single charge writing step, by sequential developments in two aqueous dispersions of oppositely charged particles. This protocol literally extends the spectra of eligible colloids that can be assembled by nanoxerography and paves the way for building complex assemblies of nanoparticles on predefined areas of surfaces, which could be useful for the elaboration of nanoparticle-based functional devices.

KEYWORDS: directed assembly · nanoxerography · colloidal nanoparticles · AFM · KFM

One of the current challenges of bottom-up nanofabrication is to precisely locate colloidal nanoparticle building blocks synthesized in liquid phase by chemical routes onto surfaces for developing nanoparticle-based functional devices. Many strategies are being explored for achieving this goal. On one side, directed assembly of colloids at the surface−liquid−gas boundary exploits the pinning of the meniscus of a liquid front moving over a smooth nonwetting surface at some specific locations, associated with the controlled convective flow of liquid toward the meniscus and capillary forces, using different setup variants.[1−3] Such pinning locations can be formed by geometric features[1,2,4,5] or wetting patterns[6−8] on the surfaces or can be induced by "stick and slip" phenomena.[9] On the other side, assembly of nanoparticles directly from the bulk liquid phase onto solid templates uses a variety of interactions such as electrostatic forces,[10] capillary forces,[11] formation of covalent bonds,[12] specific recognition between biomolecules,[13] supramolecular interactions,[14] or form factor.[15,16] Electric fields can also be applied to direct the particles toward the targeted adsorption sites.[17]

Over the past few years, nanoxerography has emerged as a versatile alternative for colloid assembly directly from the bulk liquid phase onto solid templates.[18−30] This method is a nanoscale adaptation of the industrial xerography process used in laser printing. It uses the strong electric fields generated by charge patterns written into electret thin films to trap charged and/or polarizable colloidal nanoparticles *via* electrostatic interactions. Sequential charge writing can be carried out using focused ion beam,[18] electron beam,[19] or atomic force microscopy (AFM).[20−26] The scaling up of nanoxerography can be achieved using parallel charge writing, mostly inspired by microcontact printing soft lithography.[27−32] Among the different charge writing techniques, AFM is a very versatile instrument for nanoxerography since it has the ability to perform triple functions: (i) writing of both positive and negative charges in a single run with a great flexibility on the pattern geometry, without any time-consuming nanolithography patterning of stamps, (ii) high-resolution charge imaging by surface potential measurements in the Kelvin force microscopy (KFM) electrical mode, and (iii) three-dimensional topography imaging of the resulting assemblies of nanoparticles on charge patterns.

* Address correspondence to laurence.ressier@insa-toulouse.fr.

Received for review March 30, 2011 and accepted April 20, 2011.

Published online April 20, 2011
10.1021/nn2011893

Nevertheless, directed assembly of colloids by nanoxerography is usually restricted to nanoparticles dispersed in nonpolar solvents.[18,19,21,23,30] As-synthesized aqueous colloidal dispersions are discreetly avoided since the highly polarizable water molecules screen the electric field generated by charge patterns. As a large number of colloids of different materials, shapes, sizes, and surface functionalities are prepared in aqueous medium,[33−41] this strongly restricts the range of colloidal nanoparticles that can be effectively assembled by this method. In order to circumvent this, several alternative strategies were attempted in the literature: preparation of water-in-oil emulsions,[24] use of water−alcohol mixtures,[25] transfer to low dielectric organic solvents through ligand-exchange procedures,[22] or addition of surfactants.[26] However, these approaches are very limiting and have serious drawbacks. The resolution of nanoparticle assemblies obtained with water-in-oil emulsions is strongly limited by the emulsion droplet size. Transfers to water−alcohol mixtures or low dielectric organic solvents are restricted to certain kinds of nanoparticles, and the use of surfactants leads to a contamination of the nanoparticle assemblies.

In this paper, we describe a simple protocol of AFM nanoxerography for the effective directed assembly of charged colloidal nanoparticles from aqueous dispersions without any postsynthetic processing. The assembly mechanism is understood by analyzing and comparing the evolution of the electric field generated by charge patterns in various solvents. The generic nature of this approach is then demonstrated by applying it to various types of colloids, *viz.*, latex nanoparticles, silica nanoparticles, and ligand-stabilized gold nanoparticles, ranging in size from 3 to 100 nm. Finally, directed assembly of two kinds of nanoparticles on the same surface is built using successive developments to prove the flexibility and control over geometries and complexities of nanoparticle assembly offered by this protocol.

RESULTS AND DISCUSSION

Protocol of AFM Nanoxerography. The protocol we used for directed assembly of colloidal nanoparticles from aqueous dispersions by AFM nanoxerography consists of three successive steps:

(i) AFM charge writing (Figure 1a): positive and/or negative charges are injected by means of a polarized AFM tip into 100 nm polymethylmethacrylate (PMMA) films, to create charge patterns of desired geometry. This charge writing step is performed in air under ambient conditions. It typically lasts from a few seconds to a few minutes depending on the size and complexity of the charge patterns. Just after charge writing, surface potential mappings of the charge patterns are carried out by the AFM-based electric technique of Kelvin force microscopy.[42]

(ii) Development (Figure 1b): this step consists first in incubating the desired colloidal dispersion on the electrostatically patterned samples for a certain time, t_1. The samples are then immersed in an adequate solvent called "development solvent" for a certain time, t_2. This two-stage development typically lasts between 60 and 90 s.

(iii) Drying (Figure 1c): the samples are finally dried under nitrogen flow. This step is used for removing any traces of solvent on the surface of the samples.

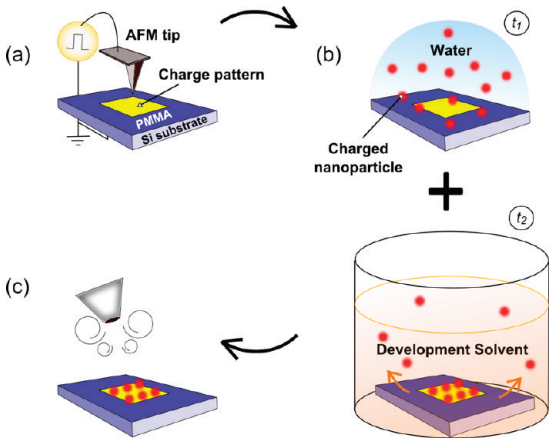

Figure 1. Schematics of the AFM nanoxerography process: (a) AFM charge writing into a 100 nm PMMA thin film; (b) two-stage development by incubation of the desired aqueous colloidal dispersion containing charged nanoparticles followed by an immersion in an adequate development solvent; (c) drying under nitrogen flow.

Two-Stage Development. In the protocols of nanoxerography reported in the literature, the development step consists only of an immersion of the electrostatically patterned samples in the desired colloidal dispersion. A subsequent rinsing is usually performed to remove nanoparticles nonselectively grafted on the surface. To demonstrate that an adequate two-stage development offers the possibility to assemble charged colloidal nanoparticles from aqueous dispersions without any postsynthetic processing, AFM nanoxerography experiments were performed on commercial, negatively charged 100 nm latex nanoparticles dispersed in water, using three development solvents of decreasing polarities (decreasing dielectric constants): Ultra high quality (UHQ) water (18 MΩ·cm), ethanol, and 2-propanol. In all cases, two 5 μm × 5 μm square patterns of opposite charge were injected by AFM into PMMA thin films. The amplitude of the voltage pulses used for charge writing was adjusted to obtain identical absolute surface potential values of 4 V (relative to the surrounding uncharged PMMA film) for either of the two charge patterns. The experimental conditions for development were identical for all experiments: a 30 μL

drop of the colloidal dispersion was deposited on the electrostatically patterned samples for t_1 = 30 s followed by immersion in the development solvent for t_2= 60 s.

Figure 2 presents typical AFM topography and KFM surface potential images of the samples after this process for the three development solvents. In the case of development with UHQ water (Figure 2a), no nanoparticle grafting is observed on the substrate surface, neither on charge patterns nor on the uncharged PMMA surface. However, the residual surface potentials of charge patterns measured by KFM are about −190 mV and +350 mV, which are normally sufficient to trap colloids dispersed in nonpolar solvents such as hexane.[23] For development with ethanol (Figure 2b), a selective single-layered assembly of latex nanoparticles is obtained on the positive charge pattern, while no nanoparticles are adsorbed anywhere else on the PMMA surface. The high lateral resolution of KFM measurements allows to distinguish latex nanoparticles grafted on the positive charge pattern and to confirm their net negative charge induced by their carboxylate functionalization. Latex nanoparticles were thus strongly grafted on the positive charge pattern and repelled by negative patterns because of Coulomb forces. In addition, a small contribution of the dielectrophoretic force to this nanoparticle assembly is evident since a denser chain of closely packed nanoparticles was formed on the edges of the positive charge pattern where the electric field gradient was stronger. The density of latex nanoparticles on the positive charge pattern is approximately 13 NPs/μm^2. In this case, the residual surface potential of the negative charge pattern measured by KFM is approximately −150 mV. In the case of development with 2-propanol (Figure 2c), a selective assembly of latex nanoparticles is observed on the positive charge pattern, but particles are also nonselectively adsorbed on the uncharged regions of the PMMA surface and a depletion area on the negative charge pattern is apparent. Once again the same conclusions made in the case of ethanol development (Figure 2b) can be drawn except that this time the density of nanoparticles over the positive charge pattern is slightly higher at 16 NPs/μm^2, and some nanoparticles (0.3 NP/μm^2) are attached on the surface outside the charge patterns. The residual surface potential of the remaining negative charge pattern measured on the KFM image is approximately −110 mV.

These experimental results clearly suggest that just after the incubation of the aqueous colloidal dispersion, an immersion in an adequate development solvent (here ethanol or 2-propanol) with a lower polarity than the nanoparticle dispersing solvent (water) allows grafting colloidal nanoparticles from aqueous dispersions onto charge patterns. It is to be noted that this protocol, demonstrated here with AFM charge writing, is evidently valid when using other charge writing techniques.

In order to understand the mechanism involved in our two-stage development, we quantified the electric field generated by charge patterns in solvents generally used in nanoxerography, employing a method that we recently published.[42] In brief, we performed numerical simulations of KFM measurements on charge patterns with the ac/dc module of the Comsol Multiphysics software taking into account side-capacitance effects induced by the tip cone and the cantilever of the scanning AFM probe. These simulations allowed us to quantify the actual surface charge density of the charge patterns. The electric fields generated by such charge patterns when immersed in different solvents were therefore estimated.

Figure 3 presents the typical evolution of the electric field generated by a 5 μm × 5 μm square charge pattern with a surface charge density of $\sigma = \pm 4.1 \times 10^{-3}$ C/m^2 (estimated from a surface potential of ±4 V relative to the uncharged surrounding PMMA film, in our KFM measurement conditions) in different media (air, Fluorinert FC-77, hexane, 2-propanol, ethanol and water), as a function of the distance in the direction perpendicular to its surface, z. As expected, the decreasing exponential evolution of $\|E\|_z$ with z strongly depends on the dielectric constant of the surrounding media. Immersion of the charge pattern in solvents of low

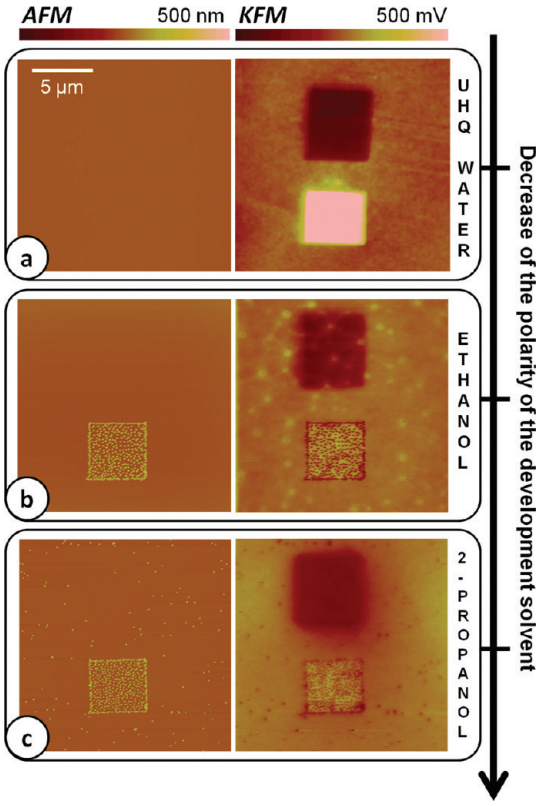

Figure 2. AFM topography (left) and corresponding KFM surface potential (right) images of directed assembly of negatively charged 100 nm latex nanoparticles dispersed in water by AFM nanoxerography using development solvents of decreasing polarities: (a) UHQ water, (b) ethanol, (c) 2-propanol.

dielectric constants (FC-77 and hexane) leads to $\|E\|_{z=0}$ values about 10 times higher than those of alcoholic ones (ethanol and 2-propanol) and 50 times higher than water. The spatial extension of the electrical field is strongly reduced in solvents of high dielectric constants. For instance, the $\|E\|_{z=0}$ value corresponding to water is obtained at $z = 4\ \mu$m for ethanol, $z = 5\ \mu$m for 2-propanol, $z = 48\ \mu$m in hexane, and $z = 50\ \mu$m in FC-77. These results suggest that during the development step of nanoxerography, the nanoparticles dispersed in water will feel much lower electric field (in both amplitude and spatial extension) of the charge patterns than nanoparticles dispersed in other solvents.

In this context, the two-stage development strategy to assemble colloids dispersed in water by nanoxerography concerns increasing the amplitude and the range of the electric field generated by charge patterns by adding alcoholic solvents, which have lower dielectric constants than water. Colloids in water are surrounded by layers of polarized water and so are the charge patterns on the substrate immersed in water. These layers of high dielectric medium considerably reduce the net charge felt by the colloids. When the electrostatically patterned samples with the deposited aqueous colloids are immersed in solvents such as ethanol or 2-propanol, the hydration layers on both the colloids and the charge patterns are destroyed by the alcohol. As a result of this, the attraction of the charged colloids to the charge patterns on the surface is facilitated and the long-range Coulomb forces lead to an instantaneous trapping of the colloids on the charge patterns. Since the volume of the alcoholic development solvent (10 mL) is much larger than the volume of the colloidal dispersion (30 μL) placed on the electrostatically patterned samples, the resulting solvent composition at the time of immersion is largely of low dielectricity constant. This situation is thus equivalent to a one-stage development

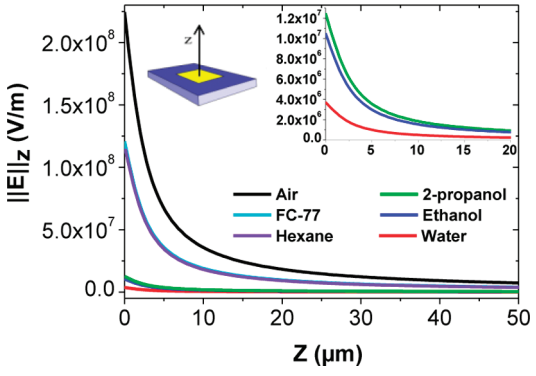

Figure 3. Spatial evolution of the amplitude of the electric field along the *z* axis $\|E\|_z$ generated by a 5 μm × 5 μm square charge pattern with a surface charge density of $\sigma = +4.1 \times 10^{-3}$ C/m^2, as a function of the surrounding media: air, FC-77, hexane, 2-propanol, ethanol, and water. Curves corresponding to FC-77 and hexane are overlaid. An enlarged plot corresponding to 2-propanol, ethanol, and water is presented in the inset.

in an alcoholic solvent. In other words, the protocol described here should yield results equivalent to those obtained using colloids dispersed in ethanol or 2-propanol. This assumption was confirmed by experimental results. Indeed, commercial carboxylate-functionalized latex nanoparticles suspended in 15% vol water in ethanol were found to assemble on charge patterns with particle densities similar to that obtained using the development of the aqueous latex colloidal dispersion in ethanol. Increasing the solvent ratio to 50% led to lower density of trapped colloids. For example, only 3 NPs/μm^2 were obtained on positive charge patterns as opposed to 13 NPs/μm^2 obtained by development in ethanol. Increasing the ratio above 65% led to no attachment of particles. Thus, this ratio is the threshold for a water−ethanol solvent mixture with which such latex nanoparticle trapping on charge patterns can be achieved. Although these findings suggest that one may use dispersions of colloids in appropriate ratios of water/alcohol for use in nanoxerography, using an appropriate alcoholic solvent in a separate subsequent sequence is advantageous. Indeed, not all colloids yield stable dispersions in water/alcohol solution ratios less than 50%, whereas performing this second stage of development can yield the best nanoparticle density on charge patterns. Of the two alcoholic development solvents used in experiments presented in Figure 2, ethanol gave the best results with no nonspecifically adsorbed particles on uncharged areas of the PMMA film. This is because latex particles have better dispersibility in ethanol as compared to 2-propanol and therefore get easily detached from the substrate.

Single and Binary Assembly of Nanoparticles. To demonstrate the versatility of our nanoxerography protocol, we applied it to assemble water-dispersible colloids of different sizes, natures, and surface functionalities on positively charged patterns of varied geometries (Figure 4). Figure 4a shows the directed assembly of 45 nm Stöber silica nanoparticles on a positive charge pattern representing an "Occitane Cross". The KFM image of this charge pattern shows that it was composed of points with a surface potential of +950 mV and a width of about 380 nm. After incubation of the dispersion of negatively charged Stöber silica nanoparticles for t_1 = 30 s and immersion in ethanol for t_2 = 30 s, the silica particles were predominantly trapped on charge points by Coulomb forces. AFM observations demonstrate the capability of selectively trapping one to three individual silica nanoparticles on each charge spot constituting this "Occitane Cross" charge pattern. Figure 4b illustrates the directed assembly of 14 nm Turkevich citrate gold nanoparticles, one of the common metallic nanoparticles known, on lines of positive charges. As shown on the KFM image, these charge lines had a surface potential of +750 mV and were approximatively 320 nm wide. After incubation of the dispersion of negatively charged citrate

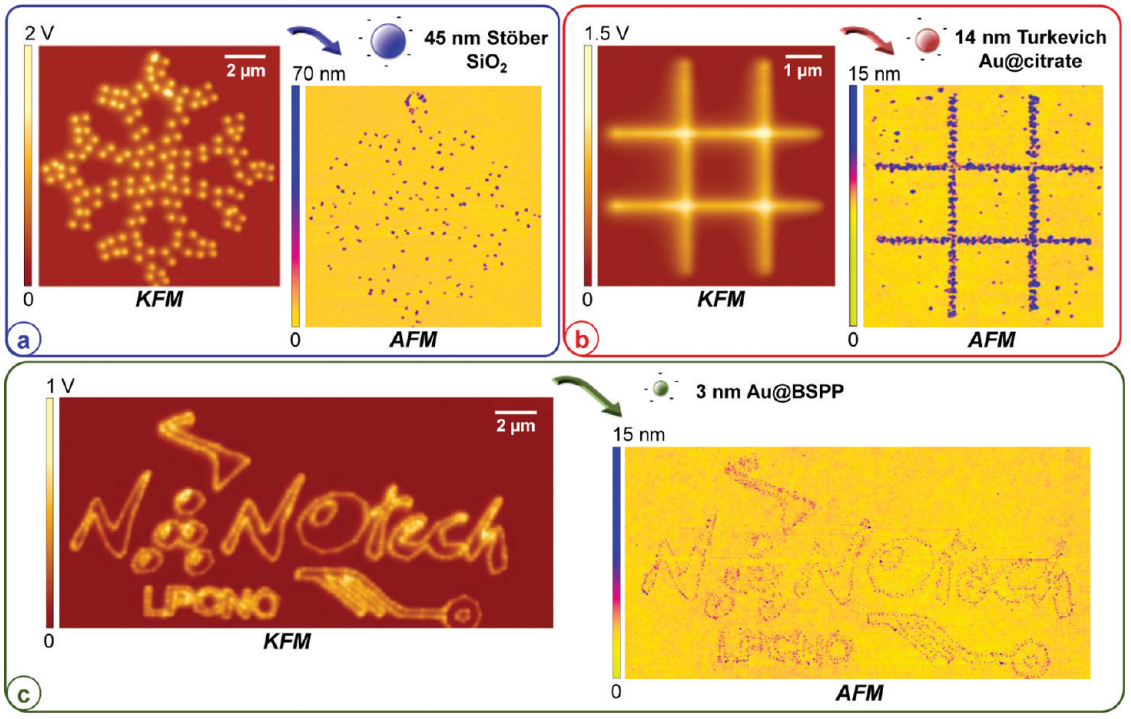

Figure 4. KFM surface potential images (left) of positive charge patterns of varied geometries and AFM topography images in tapping mode (right) of directed assemblies of various kinds of water-dispersed colloidal nanoparticles on these patterns: (a) 45 nm Stöber silica nanoparticles, (b) 14 nm Turkevich gold nanoparticles, (c) 3 nm BSPP-stabilized gold nanoparticles.

gold nanoparticles for t_1 = 30 s and immersion in ethanol for t_2 = 30 s, 200 nm wide nanoparticle lines appeared on the charge lines, once again due to Coulomb interactions. Figure 4c illustrates the directed assembly of smaller, 3 nm gold nanoparticles stabilized by bis(*p*-sulfonatophenyl) phenylphosphine (BSPP) on a positive charge pattern representing the logo of our research group "Nanotech". The KFM image shows that the surface potential of this charge pattern was about +400 mV with a line width of about 200 nm. After incubation of the dispersion of negatively charged 3 nm gold nanoparticles for t_1 = 30 s and immersion in ethanol for t_2 = 30 s, a single layer of gold particles was selectively trapped on the charge pattern, directed by Coulomb attraction. AFM observations reveal that the high degree of pattern complexity was preserved with an average line width of about 50 nm, proving the efficiency of the protocol.

Moreover, this AFM nanoxerography protocol offers the opportunity to achieve directed assembly of two kinds of nanoparticles carrying opposite charges by successive developments from individual colloidal dispersions using charge patterns written by AFM. Figure 5 presents a typical example of such a directed binary assembly on the same surface by AFM nanoxerography. The KFM image on the left shows a charge pattern representing the map of France, obtained in the same run of charge writing, where the left half was positively charged (surface potential of +800 mV, line width of about 350 nm) and the right negatively charged (surface potential of −600 mV, line width of about 400 nm). After incubation of a dispersion of 100 nm negatively charged latex nanoparticles on this oppositely charged pattern for a duration of t_1 = 30 s followed by an immersion in ethanol for t_2 = 30 s and a simple drying under nitrogen flow, an incubation of a dispersion of 8 nm positively charged gold nanoparticles stabilized with the cationic poly[(3-acrylamidopropyl) trimethylammonium chloride] (PAPTAC) polymer during t_1 = 30 s followed by an immersion in 2-propanol for t_2 = 30 s was performed. The AFM image in Figure 5 confirms the success of this binary assembly of nanoparticles, showing a line of individual 100 nm latex nanoparticles on the left part of the charge pattern and a 190 nm wide single-layered line of gold nanoparticles on the right. This binary assembly of nanoparticles is dense enough to be observed by optical microscopy, which could be useful for further processing of the nanoparticle assembly or for alignments. To our knowledge, this is the first example of serial deposition of oppositely charged nanoparticles by nanoxerography. It testifies the fact that Coulomb forces drive the nanoparticle assembly in this protocol. This kind of binary assembly of nanoparticles could not be achieved from uncharged polarizable nanoparticles, because in this case, the dominant dielectrophoretic forces would lead to nanoparticle deposition on patterns of opposite charges at the same time.[23] Significantly, these results prove that the surface potential of the negatively charged part of the pattern was preserved through the first development with latex colloidal dispersion and is strong enough to

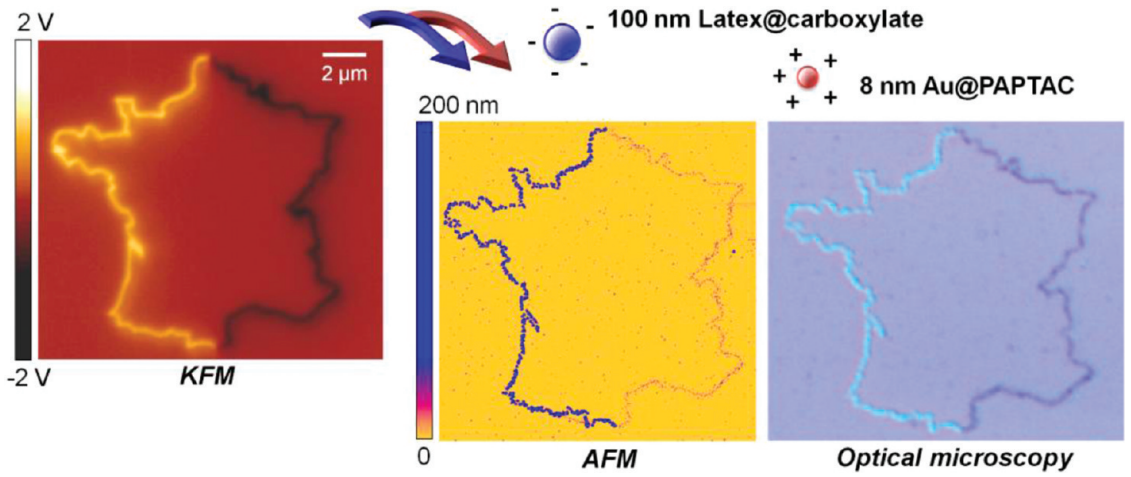

Figure 5. KFM surface potential image (left) of a charge pattern representing the map of France where the left half was positively charged and the right half was negatively charged. AFM topography image in tapping mode (middle) and optical microscopy image in bright field (right) of directed assembly of negatively charged 100 nm latex nanoparticles and positively charged 8 nm PAPTAC polymer stabilized gold nanoparticles on this pattern obtained by successive developments in the two colloidal dispersions.

be used to trap the positively charged gold nanoparticles during the subsequent development. They also demonstrate the robustness of colloidal grafting on charge patterns since it is not modified by a second development.

From all these results, a few general comments concerning the nanoparticle assembly by this protocol of AFM nanoxerography can be made. In all cases only a single layer of nanoparticles is grafted on charge patterns, indicating that the screening of charge patterns by the first nanoparticle layer avoids the grafting of a second one. The lateral resolution of nanoparticle assembly mainly depends on the charge density and width of charge patterns, together with the charge density and concentration of nanoparticles in the dispersion. The selectivity of the nanoparticle assembly is determined by the affinity of the nanoparticles to the electret thin film surface and the dispersibility of nanoparticles in the development solvent.

CONCLUSIONS

Ever since the first experiments of nanoxerography, as-synthesized aqueous colloidal dispersions were avoided to prevent the screening of the electric field of the charge patterns by the high dielectric water molecules. To overcome this drawback, we have developed a simple and reliable protocol to assemble charged nanoparticles from aqueous dispersions by nanoxerography in a few minutes. It involves a two-stage development based on an immersion in an appropriate water-soluble alcohol solvent just after the incubation of the colloidal dispersion of interest on the electrostatically patterned samples.

The immersion in an alcoholic solvent which has a lower dielectric constant compared to water helps in increasing the amplitude and the range of the electric field generated by charge patterns to facilitate the electrostatic attraction of charged colloids. This protocol, demonstrated here with AFM charge writing, can be extended to colloidal nanoxerography using other charge writing techniques and allows the use of a wide range of water-dispersible colloidal nanoparticles without any postsynthetic processing.

The generic nature of this protocol to assemble charged nanoparticles from aqueous dispersions by nanoxerography was demonstrated by constructing various assemblies of charged organic/inorganic/metallic (latex, silica, gold) nanoparticles of different sizes (3 to 100 nm) and surface functionalities from aqueous dispersions on charge patterns of varied geometries. The protocol even offers the ability to serially deposit oppositely charged nanoparticles on geometrical patterns of both charges written by AFM in a single run.

This work demonstrates the high potential of AFM nanoxerography for single and binary directed assembly of colloids on patterns of unrestricted geometries since it combines rapidity and versatility. It paves the way for building nanoparticle architectures of desired complexity and fabricating novel nanoparticle-based functional devices.

METHODS

Colloidal Nanoparticles. *Latex Nanoparticles.* Latex nanoparticles dispersed in water were purchased from Polysciences, Inc. The commercial dispersion was diluted in deionized water to obtain a concentration of 2×10^{11} NPs/mL. Transmission electron microscopy (TEM) analysis of the dispersion indicated the presence of 100 ± 8 nm spherical latex particles. Zeta potential measurements revealed that these latex nanoparticles carried a net negative charge $\xi = -45$ mV. This net negative charge was due to their surface functionalization with carboxylate groups.

Silica Nanoparticles. Silica nanoparticles were synthesized by the Stöber method.[35,43] To a solution of 5.7 mL of 25%

aqueous ammonia were added 114 mL of absolute ethanol and 3.8 mL of tetraethyl orthosilicate, and the solution was stirred overnight. The turbid dispersion of silica nanoparticles obtained was centrifuged to obtain a white pellet of the nanoparticles. This was washed three times with ethanol and once with water and finally redispersed in deionized water. The final concentration of silica nanoparticles in the dispersion was about 3×10^{11} NPs/mL. TEM analysis of the dispersion indicated the presence of 45 ± 3 nm spherical silica particles. Zeta potential measurements revealed that these silica nanoparticles carried a net negative charge $\xi = -21$ mV. This negative charge was due to the presence of $-$Si-O$^-$ groups on their surface.

Citrate-Stabilized Gold Nanoparticles. Citrate-stabilized gold nanoparticles were synthesized by the Turkevich–Frens method.[36,44,45] A boiling solution of sodium citrate (62 mg, 0.240 mmol) in 5 mL of water was added to a boiling solution of $HAuCl_4$ (10 mg, 0.025 mmol) in 60 mL of water. The color of the solution turned red after 10 min, indicating the formation of gold nanoparticles. This was boiled further for 15 min, cooled to room temperature, and finally diluted with deionized water. The final concentration of gold nanoparticles in the dispersion was about 2×10^{11} NPs/mL. TEM analysis of the dispersion indicated the presence of 14 ± 1 nm particles. Zeta potential measurements revealed that these gold nanoparticles carried a net negative charge $\xi = -35$ mV. This negative charge of these NPs was due to the citrate molecules bound to their surface.

BSPP-Stabilized Gold Nanoparticles. Bis(*p*-sulfonatophenyl) phenylphosphine (BSPP)-stabilized gold nanoparticles were synthesized by a typical $NaBH_4$ reduction. Specifically, a 20 mL aqueous solution of $HAuCl_4$ (2.5×10^{-4} mol L^{-1}) and BSPP (2.5×10^{-4} mol L^{-1}) was stirred vigorously at 30 °C. To this was injected 0.6 mL of a freshly prepared ice cold aqueous solution of $NaBH_4$ (0.1 mol L^{-1}). The color of the mixture immediately turned yellowish-brown, indicating the formation of small gold nanoparticles. Stirring was stopped after 10 s, and the solution was aged for 2 h at 30 °C. The final concentration of gold nanoparticles in the dispersion diluted with deionized water was about 5×10^{10} NPs/mL. TEM analysis of the dispersion indicated the presence of 3 ± 1 nm spherical particles. Zeta potential measurements revealed that these gold nanoparticles carried a net negative charge $\xi = -17$ mV. This negative charge was due to BSPP molecules complexed to their surface.

PAPTAC-Stabilized Gold Nanoparticles. Positively charged stabilized nanoparticles were prepared by coating separately synthesized gold nanoparticles with a given amount of the cationic poly[(3-acrylamidopropyl) trimethylammonium chloride] polymer. Briefly, to 5 mL of $HAuCl_4$ solution (1×10^{-2} mol L^{-1}) were added 94 mL of deionized water and 250 μL of aqueous NaOH (1 mol·L^{-1}), and the pH of this solution was adjusted between 7.5 and 8. Then 500 μL of fresh aqueous $NaBH_4$ solution (0.1 mol L^{-1}) was added under stirring. The color of the suspension immediately turned dark red, indicating the formation of gold nanoparticles. TEM analysis of the dispersion indicated the presence of 8 ± 2 nm spherical particles. To 1 mL of these preformed nanoparticles was added 1 mL of a 0.01 wt % aqueous stock solution of PAPTAC synthesized as previously described[46] and chosen with an average molar mass of 10 000 g·mol^{-1} ([Au^0] = 2.5×10^{-4} mol L^{-1}; [PAPTAC polymer] = 5×10^{-3} wt %) . After dialysis, zeta potential measurements revealed that these nanoparticles carried a net positive charge $\xi = +33$ mV. This positive charge was due to their coating by the cationic PAPTAC polymer.

AFM Charge Writing. Charge writing was performed on 100 nm PMMA thin films spin-coated on *p*-doped (10^{16} cm^{-3}) silicon wafers, by applying voltage pulses with an external generator to a highly *n*-doped silicon AFM tip (resonance frequency of 290 kHz), using home-written tip guiding software. The *z*-feedback was adjusted to control the tip–sample interaction during charge writing. The width and the frequency of voltage pulses were fixed at 1 ms and 50 Hz, respectively. The pulse amplitude was varied between 40 and 75 V depending on the written charge pattern. The tip velocity was fixed at 10 μm/s for all experiments. These specific writing conditions were chosen because of their reliability and reproducibility, without any tip and/or sample damage at the high voltages used, as demonstrated in our previous work.[47] All experiments were performed in air under ambient conditions (temperature of 22–25 °C, relative humidity of 40–50%), using an ICON atomic force microscope from Veeco Instruments.

KFM Charge Imaging. Just after AFM charge writing, surface potential mappings of charge patterns were performed in air by amplitude modulation KFM using the same microscope and the same probe. These KFM measurements were carried out using the "lift" technique at a constant lift height of 30 nm. A fixed drive amplitude V_{AC} of 3 V was chosen to make sensitive potential measurements while avoiding any parametric amplification. The surface potential (relative to the surrounding uncharged PMMA film) and the width of the written charge patterns were systematically extracted from KFM images. In our experimental conditions, the lateral resolution of KFM measurements was about 50–100 nm (limited by the long-range nature of electrostatic forces) with a potential noise of about 5 mV.

Acknowledgment. We thank G. Delamare for his valuable help in the development of the home-written tip guiding software used for charge writing. This work was supported by the French National Agency (ANR) in the framework of its program "Nanosciences, Nanotechnologies and Nanosystems (P3N2009)" (AUBAINE project no. ANR-09-NANO-036).

REFERENCES AND NOTES

1. Maury, P.; Escalante, M.; Reinhoudt, D. N.; Huskens, J. Directed Assembly of Nanoparticles onto Polymer-Imprinted or Chemically Patterned Templates Fabricated by Nanoimprint Lithography. *Adv. Mater.* **2005**, *17*, 2718–2723.
2. Yin, Y.; Lu, Y.; Gates, B.; Xia, Y. Template-Assisted Self-Assembly. *J. Am. Chem. Soc.* **2001**, *123*, 8718–8729.
3. Malaquin, L.; Kraus, T.; Schmid, H.; Delamarche, E.; Wolf, H. Controlled Particle Placement Through Convective and Capillary Assembly. *Langmuir* **2007**, *23*, 11513–11521.
4. Cui, Y.; Björk, M. T.; Liddle, J. A.; Sönnichsen, C.; Boussert, B.; Alivisatos, A. P. Integration of Colloidal Nanocrystals into Lithographically Patterned Devices. *Nano Lett.* **2004**, *4*, 1093–1098.
5. Fustin, C. A.; Glasser, G.; Spiess, H. W.; Jonas, U. Parameters Influencing the Templated Growth of Colloidal Crystals on Chemically Patterned Surfaces. *Langmuir* **2004**, *20*, 9114–9123.
6. Viallet, B.; Ressier, L.; Czornomaz, L.; Decorde, N. Tunable Pyramidal Assemblies of Nanoparticles by Convective/Capillary Deposition on Hydrophilic Patterns Made by AFM Oxidation Lithography. *Langmuir* **2010**, *26*, 4631–4634.
7. Fustin, C. A.; Glasser, G.; Spiess, H. W.; Jonas, U. Site-Selective Growth of Colloidal Crystals with Photonic Properties on Chemically Patterned Surfaces. *Adv. Mater.* **2003**, *15*, 1025–1028.
8. Xia, Y.; Whitesides, G. M. Soft Lithography. *Annu. Rev. Mater. Sci.* **1998**, *28*, 153–184.
9. Farcau, C.; Moreira, H.; Viallet, B.; Grisolia, J.; Ressier, L. Tunable Conductive Nanoparticle Wire Arrays Fabricated by Convective Self-Assembly on Nonpatterned Substrates. *ACS Nano* **2010**, *4*, 7275–7282.
10. Lee, I.; Zheng, H.; Rubner, M. F.; Hammond, P. T. Controlled Cluster Size in Patterned Particle Arrays *via* Directed Adsorption on Confined Surfaces. *Adv. Mater.* **2002**, *14*, 572–577.
11. Srinivasan, U.; Liepmann, D.; Howe, R. T. Microstructure to Substrate Self-Assembly Using Capillary Forces. *J. Microelectromech. Syst.* **2001**, *10*, 17–24.
12. Liu, S.; Maoz, R.; Schmid, G.; Sagiv, J. Template Guided Self-Assembly of [Au55] Clusters on Nanolithographically Defined Monolayer Patterns. *Nano Lett.* **2002**, *2*, 1055–1060.
13. Le, J. D.; Pinto, Y.; Seeman, N. C.; Musier-Forsyth, K.; Taton, T. A.; Kiehl, R. A. DNA-Templated Self-Assembly of Metallic Nanocomponent Arrays on a Surface. *Nano Lett.* **2004**, *4*, 2343–2347.
14. Maury, P.; Péter, M.; Crespo-Biel, O.; Ling, X. Y.; Reinhoudt, D. N.; Huskens, J. Patterning the Molecular Printboard. *Nanotechnology* **2007**, *18*, 044007.

15. Yeh, H. J. J.; Smith, J. S. Fluidic Self-Assembly for the Integration of GaAs Light-Emitting Diodes on Si Substrates. *Photonics Technol. Lett., IEEE* **1994**, *6*, 706–708.
16. Talghader, J. J.; Tu, J. K.; Smith, J. S. Integration of Fluidically Self-Assembled Optoelectronic Devices Using a Silicon-Based Process. *Photonics Technol. Lett., IEEE* **1995**, *7*, 1321–1323.
17. Li, M.; Bhiladvala, R. B.; Morrow, T. J.; Sioss, J. A.; Lew, K. K.; Redwing, J. M.; Keating, C. D.; Mayer, T. S. Bottom-up Assembly of Large-Area Nanowire Resonator Arrays. *Nat. Nanotechnol.* **2008**, *3*, 88–92.
18. Fudouzi, H.; Kobayashi, M.; Shinya, N. Site-Controlled Deposition of Microsized Particles Using an Electrostatic Assembly. *Adv. Mater.* **2002**, *14*, 1649–1652.
19. Fudouzi, H.; Kobayashi, M.; Shinya, N. Assembling 100 nm Scale Particles by an Electrostatic Potential Field. *J. Nanopart. Res.* **2001**, *3*, 193–200.
20. Mesquida, P.; Stemmer, A. Attaching Silica Nanoparticles from Suspension onto Surface Charge Patterns Generated by a Conductive Atomic Force Microscope Tip. *Adv. Mater.* **2001**, *13*, 1395–1398.
21. Tzeng, S. D.; Lin, K. J.; Hu, J. C.; Chen, L. J.; Gwo, S. Templated Self-Assembly of Colloidal Nanoparticles Controlled by Electrostatic Nanopatterning on a $Si_3N_4/SiO_2/Si$ Electret. *Adv. Mater.* **2006**, *18*, 1147–1151.
22. Ressier, L.; Palleau, E.; Garcia, C.; Viau, G.; Viallet, B. How to Control AFM Nanoxerography for the Templated Monolayered Assembly of 2 nm Colloidal Gold Nanoparticles. *Nanotechnol., IEEE Trans.* **2009**, *8*, 487–491.
23. Palleau, E.; Ressier, L. Assembly Mechanisms of 10 nm Colloidal Silver Nanoparticles by AFM Nanoxerography. *J. Nanosci. Nanotechnol.* **2010**, in press.
24. Naujoks, N.; Stemmer, A. Micro- and Nanoxerography in Liquids-Controlling Pattern Definition. *Microelectron. Eng.* **2005**, *78*, 331–337.
25. Seemann, L.; Stemmer, A.; Naujoks, N. Selective Deposition of Functionalized Nano-Objects by Nanoxerography. *Microelectron. Eng.* **2007**, *84*, 1423–1426.
26. Seemann, L.; Stemmer, A.; Naujoks, N. Local Surface Charges Direct the Deposition of Carbon Nanotubes and Fullerenes into Nanoscale Patterns. *Nano Lett.* **2007**, *7*, 3007–3012.
27. Zhao, D.; Duan, L.; Xue, M.; Ni, W.; Cao, T. Patterning of Electrostatic Charge on Electrets Using Hot Microcontact Printing. *Angew. Chem., Int. Ed.* **2009**, *48*, 6699–6703.
28. Ma, X.; Zhao, D.; Xue, M.; Wang, H.; Cao, T. Selective Discharge of Electrostatic Charges on Electrets Using a Patterned Hydrogel Stamp. *Angew. Chem., Int. Ed.* **2010**, *49*, 5537–5540.
29. Jacobs, H. O.; Whitesides, G. M. Submicrometer Patterning of Charge in Thin-Film Electrets. *Science* **2001**, *291*, 1763–1766.
30. Jacobs, H. O.; Campbell, S. A.; Steward, M. G. Approaching Nanoxerography. *Adv. Mater.* **2002**, *14*, 1553–1557.
31. Barry, C. R.; Jacobs, H. O. Fringing Field Directed Assembly of Nanomaterials. *Nano Lett.* **2006**, *6*, 2790–2796.
32. Cole, J. J.; Barry, C. R.; Wang, X.; Jacobs, H. O. Nanocontact Electrification Through Forced Delamination of Dielectric Interfaces. *ACS Nano* **2010**, *4*, 7492−7498.
33. Jana, N. R.; Gearheart, L.; Murphy, C. J. Wet Chemical Synthesis of High Aspect Ratio Cylindrical Gold Nanorods. *J. Phys. Chem. B* **2001**, *105*, 4065–4067.
34. Tao, A. R.; Habas, S.; Yang, P. Shape Control of Colloidal Metal Nanocrystals. *Small* **2008**, *4*, 310–325.
35. Stober, W.; Fink, A.; Bohn, E. Controlled Growth of Monodisperse Silica Spheres in the Micron Size Range. *J. Colloid Interface Sci.* **1968**, *26*, 62–69.
36. Enüstün, B. V.; Turkevich, J. Coagulation of Colloidal Gold. *J. Am. Chem. Soc.* **1963**, *85*, 3317–3328.
37. Dahl, J. A.; Maddux, B. L. S.; Hutchison, J. E. Toward Greener Nanosynthesis. *Chem. Rev.* **2007**, *107*, 2228–2269.
38. Stoeva, S. I.; Smetana, A. B.; Sorensen, C. M.; Klabunde, K. J. Gram-Scale Synthesis of Aqueous Gold Colloids Stabilized by Various Ligands. *J. Colloid Interface Sci.* **2007**, *309*, 94–98.
39. Dong, H.; Lee, S. Y.; Yi, G. R. Controlling the Size and Surface Morphology of Carboxylated Polystyrene Latex Particles by Ammonium Hydroxide in Emulsifier-Free Polymerization. *Macromol. Res.* **2009**, *17*, 397–402.
40. Qu, H.; Caruntu, D.; Liu, H.; O'Connor, C. J. Water-Dispersible Iron Oxide Magnetic Nanoparticles with Versatile Surface Functionalities. *Langmuir* **2011**, *27*, 2271–2278.
41. Pons, T.; Lequeux, N.; Mahler, B.; Sasnouski, S.; Fragola, A.; Dubertret, B. Synthesis of Near-Infrared-Emitting, Water-Soluble CdTeSe/CdZnS Core/Shell Quantum Dots. *Chem. Mater.* **2009**, *21*, 1418–1424.
42. Palleau, E.; Ressier, L.; Borowik, Ł; Mélin, T. Numerical Simulations for a Quantitative Analysis of AFM ElectrostaticNanopatterning on PMMA by Kelvin Force Microscopy. *Nanotechnology* **2010**, *21*, 225706.
43. Hiramatsu, H.; Osterloh, F. E. pH-Controlled Assembly and Disassembly of Electrostatically Linked $CdSe-SiO_2$ and $Au-SiO_2$ Nanoparticle Clusters. *Langmuir* **2003**, *19*, 7003–7011.
44. Stevenson, P. C.; Hillier, J.; Turkevich A Study of the Nucleation and Growth Processes in the Synthesis of Colloidal Gold. *Discuss. Faraday Soc.* **1951**, *11*, 55–75.
45. Frens, G. Controlled Nucleation for the Regulation of the Particle Size in Monodisperse Gold Solutions. *Nat. Phys. Sci.* **1973**, *241*, 20–22.
46. Beija, M.; Palleau, E.; Sistach, S.; Zhao, X.; Ressier, L.; Mingotaud, C.; Destarac, M.; Marty, J.-D. Control of the Catalytic Properties and Directed Assembly on Surfaces of MADIX/RAFT Polymer-Coated Gold Nanoparticles by Tuning Polymeric Shell Charge. *J. Mater. Chem.* **2010**, *20*, 9433–9442.
47. Ressier, L.; Nader, V. L. Electrostatic Nanopatterning of PMMA by AFM Charge Writing for Directed Nano-Assembly. *Nanotechnology* **2008**, *19*, 135301.